

Quantum Entanglement and Information Processing via Excitons in Optically-Driven Quantum Dots

John H. Reina[†], Luis Quiroga[‡], and Neil F. Johnson[†]

[†]*Physics Department, Clarendon Laboratory, Oxford University, Oxford, OX1 3PU, U.K.*

[‡]*Departamento de Física, Universidad de Los Andes, Santafé de Bogotá, A.A. 4976, Colombia*

(February 22, 2019)

Abstract

We show how optically-driven coupled quantum dots can be used to prepare maximally entangled Bell and Greenberger-Horne-Zeilinger states. Manipulation of the strength and duration of the selective light-pulses needed for producing these highly entangled states provides us with crucial elements for the processing of solid-state based quantum information. Theoretical predictions show that several hundred single quantum bit rotations and Controlled-Not gates can be performed before decoherence of the excitonic states takes place.

I. INTRODUCTION

Quantum computation, quantum communication, quantum cryptography and quantum teleportation [1–5] are some of the most exciting applications of the fundamental principles of quantum theory. Since the seminal idea of Feynman in 1982 concerning the possibility of constructing a new generation of computers -the quantum mechanical ones [1]- and the work of Deutsch in 1985 [2], who showed, by introducing the first model of a quantum mechanical Turing machine, that this kind of computer could be constructed, research in the field of both pure and applied processing of quantum information has been widely studied and we now have the greatest magnitude of technological challenge ever. In addition, and opening the way to new fast quantum searching algorithms, in 1994, Shor [6] discovered that a quantum computer can factorize large integers. Two years later the proof that quantum error-correcting codes exist arrived [7]. Up until now, such quantum mechanical computers have been proposed in terms of trapped ions and atoms [8], cavity quantum electrodynamics (QED) [9], nuclear magnetic resonance [10], Josephson junctions [11] and semiconductor nanostructures [12] schemes. All of the above proposals have decoherence and operational errors as the main obstacles for their experimental realization, which pose much stronger problems here than in classical computers.

There is much current excitement about the possibility of using solid-state based devices in the achievement of quantum computation tasks. Particularly, the very well developed semiconductor nanostructures fabrication technology offers us a wide and promising arena in the challenging project of quantum information processing. This fact makes of semiconductor quantum dots (QDs), and because its quantum mechanical nature and its potential scalability properties, very promising candidates in the implementation of quantum computing processes. Next, we briefly review the solid state practical design schemes for quantum computation proposed to date: Kane [12] has proposed a scheme which encodes information onto the nuclear spins of donor atoms in doped silicon electronic devices where externally applied electric fields are used to perform logical operations on individual spins.

Burkard *et al.* [12] have presented a scheme based on electron spin effects, in which coupled quantum dots are used as a quantum gate. This scheme is based on the fact that the electron spins on the dots have an exchange interaction J which changes sign with increasing external magnetic field. Possible quantum gate implementations have been proposed by Barenco *et al.* [12] by considering electronic charge effects in coupled QDs, however this scheme has as the main disadvantage rapid phonon decoherence, if compared with the above proposals. More recently, Imamoglu *et al.* [12] have considered a quantum computer model based on both electron spins and cavity QED which is capable of realizing controlled interactions between two distant QD spins. In their model, the effective long-range interaction is mediated by the vacuum field of a high finesse microcavity, and single quantum bit (qubit) rotations and Controlled-Not (CNOT) operations are realized by using electron-hole Raman transitions induced by classical laser fields and the cavity mode. To our knowledge, the last proposal for quantum computing in solid state schemes is that of Vrijen *et al.* [12], which considered electron spin resonance transistors in Silicon-Germanium heterostructures: one and two qubit operations are performed by applying a gate bias.

In this paper we will focus on an optically-driven coupled QDs proposal in order to perform reliable highly entangled states of excitons and so provide a mechanism for processing quantum information over a reasonable parameter window, before decoherence of the excitonic states takes place. In the physical implementation of the quantum entanglement scheme proposed here, we exploit recent experimental results involving *coherent optical control* of excitons in single quantum dots on the nanometer and femtosecond scales [13–15]. The amazing degree of control of the quantum states of these individual “artificial atoms” [13] due to the manipulation of the confined state wave function of a single dot is an exciting and promising development with the potential for performing large scale quantum computing. As one exciton can be trapped in the dot, we have the direct possibility to use QDs as elements with *quantum memory* capacity in quantum computation operations, through a precise and controlled excitation of the system. As it is demonstrated in [13], it is possible to excite and probe *only one* individual QD within a broad distribution of dots,

with the important result that the dephasing time is much longer in a single dot (40ps) than in the bulk semiconductors (< 1 ps) studied before. Hence, new experimental possibilities in the achievement of much longer intrinsic coherence times are of current availability, fact of fundamental importance if looking towards the practical implementation of single qubit rotations and quantum CNOT gates, crucial elements for carry out quantum information processing tasks.

The outline of this paper is as follows: Section II gives a detailed description of the coupling of qubits (i.e. QDs) to pulses of light and the generation of maximally entangled Bell (or EPR) [16,17] and Greenberger-Horne-Zeilinger (GHZ) [18] states in systems comprising two and three quantum dots, respectively. The discussion of the results and experimental considerations are presented in Section III. In Section IV we review the required elements for performing quantum computation tasks and the links with the solid state set-up proposed here. Conclusions are given in Section V.

II. COUPLING OF QUBITS TO PULSES OF LIGHT AND THE GENERATION OF MAXIMALLY ENTANGLED STATES

A. The Analytical Solution

The existence of entangled states rests on the basis of quantum mechanics. Quantum entanglement is of fundamental interest since many of the most basic aspects of quantum theory require its successful generation and manipulation. Hence, the controlled generation of entanglement is highly desirable; in particular Bell and GHZ maximally entangled states are the starting point for fundamental discussions such as the violation of Bell's inequalities [19] and the non-locality problem [17], as well as for teleportation [5] and quantum cryptography [4]. Here we will show how to generate maximally entangled states of two and three qubits of the form $|\Psi_{Bell}\rangle = \frac{1}{\sqrt{2}}(|00\rangle + e^{i\varphi}|11\rangle)$ and $|\Psi_{GHZ}\rangle = \frac{1}{\sqrt{2}}(|000\rangle + e^{i\varphi}|111\rangle)$, for arbitrary values of the phase factor φ [20], taking into account a semiconductor nanostructure set-

up. In this model we consider a system of N identical and equispaced QDs, containing no net charge, which are radiated by long-wavelength classical light. Hence formation of single excitons within the individual QDs and their inter-dot transfer can be described, in the frame of the *rotating wave approximation* (RWA), by the Hamiltonian [21,22] ($\hbar = 1$ throughout this paper):

$$H(t) = \frac{1}{2}\epsilon \sum_{p=1}^N \{c_p^\dagger c_p - h_p h_p^\dagger\} + \frac{1}{2}W \sum_{p,p'=1}^N \{c_p^\dagger h_{p'} c_{p'} h_{p'}^\dagger + h_p c_{p'}^\dagger h_{p'}^\dagger c_{p'}\} + \xi(t) \sum_{p=1}^N c_p^\dagger h_p^\dagger + \xi^*(t) \sum_{p=1}^N h_p c_p, \quad (1)$$

where c_p^\dagger (h_p^\dagger) is the electron (hole) creation operator in the p th quantum dot, ϵ is the QD band gap, W the interdot interaction, and $\xi(t)$ the laser pulse shape. The terms involved in Eq. (1) obey the anticommutation rules $\{c_{p'}, c_p^\dagger\} = \{h_{p'}, h_p^\dagger\} = \delta_{pp'}$. By introducing the operators

$$J_+ = \sum_{p=1}^N c_p^\dagger h_p^\dagger, \quad J_- = \sum_{p=1}^N h_p c_p, \quad J_Z = \frac{1}{2} \sum_{p=1}^N \{c_p^\dagger c_p - h_p h_p^\dagger\}, \quad (2)$$

Eq. (1) adopts the structure

$$H(t) = H_0 + H_L(t), \quad (3)$$

where

$$H_0 = \epsilon J_Z + W(J^2 - J_Z^2), \quad \text{and} \quad H_L(t) = \xi(t) J_+ + \xi^*(t) J_-, \quad (4)$$

with $J^2 \equiv \frac{1}{2}[J_+ J_- + J_- J_+] + J_Z^2$, and the J_i -operators obeying the usual angular momentum commutation relations $[J_Z, J_\pm] = \pm J_\pm$, $[J_+, J_-] = 2J_Z$, and $[J^2, J_+] = [J^2, J_-] = [J^2, J_Z] = 0$. Hence the quantum dynamical problem associated with the time evolution of any initial state under the action of $H(t)$ is described by:

$$i\partial_t |\Psi(t)\rangle_S = \{H_0 + H_L(t)\} |\Psi(t)\rangle_S, \quad (5)$$

where the subscript S indicates Schrödinger picture. We consider the laser pulse shape like $\xi(t) = A e^{-i\omega t}$, where A gives the electron-photon coupling and the incident electric field strength. We also introduce the unitary transformation $\Lambda(t) = e^{-i\omega J_Z t}$, whose application, in the Schrödinger picture, leads us from the *laboratory frame* (LF) to the *rotating frame*

(RF) by using the rule $|\Psi(t)\rangle_\Lambda = \Lambda^\dagger(t) |\Psi(t)\rangle_S$. Hence, Eq. (5) may be rewritten as:

$$i\partial_t |\Psi(t)\rangle_\Lambda = H' |\Psi(t)\rangle_\Lambda , \quad (6)$$

with

$$H' = \Delta_\omega J_Z + W(J^2 - J_Z^2) + AJ_+ + A^*J_- . \quad (7)$$

Here $\Delta_\omega \equiv \epsilon - \omega$ is the detuning parameter. We note the importance of the Λ -transformation: the new Hamiltonian H' is time-independent. From a practical point of view, parameters A and Δ_ω are adjustable in the experiment to have control over the system of QDs (or qubits). Since J^2 commutes with the operators J_\pm , H' may be diagonalized separately in each one of these J -subspaces. Consider the $\{J, q\}$ subspace spanned by $|M\rangle \equiv |J, M; q\rangle$: the only possible values for J are $\frac{N}{2}, \frac{N}{2} - 1, \dots, \frac{1}{2}$ or 0, and per each J -fixed value, we have $2J+1$ different values for M , which are given by $M = -\frac{N}{2}, -\frac{N}{2} + 1, \dots, \frac{N}{2} - 1, \frac{N}{2}$. We introduce the label q to further distinguish the states: $q = 1, 2, \dots, D_J$, where the multiplicity D_J , i.e. the number of states having angular momentum J and $M = J$, is given by $D_J = \frac{2J+1}{J+\frac{N}{2}+1} \left(\frac{N}{2}+J\right)$. The product states $\prod_{k=1}^N |m_k\rangle \equiv |m_1, \dots, m_N\rangle$ with $J_Z = \sum_k m_k$ form a 2^N -dimensional basis which expand the Hilbert space $SU(2)^{\otimes N}$. In this basis, the 2^N eigenvalues of H' are obtained by diagonalizing the Hamiltonian matrix of elements $\langle J, M, q | H' | J', M', q' \rangle$. We get the non-zero elements as follows:

$$\begin{aligned} \langle M | H' | M' \rangle \equiv H'_{MM'} &= \left(\Delta_\omega M + W \left[J(J+1) - M^2 \right] \right) \delta_{M,M'} + \\ &+ A\sqrt{J(J+1) - M'(M'+1)} \delta_{M,M'+1} + A^*\sqrt{J(J+1) - M'(M'-1)} \delta_{M,M'-1} . \end{aligned} \quad (8)$$

The matrix elements given in Eq. (8) provide us with the general rule for any number of QDs. Since the right side of this equation does not depend on q we only need to diagonalize a square matrix of side $2J+1$ for each J . Every eigenvalue so obtained occurs D_J times in the entire spectrum. Next, we will show that solution of the eigenfunction problem associated with Eq. (8) leads to the generation of highly N -entangled states of excitons in QDs.

1. Coupling of $N=2$ QDs and Generation of Bell States

In this section we describe the procedure for the generation of entangled Bell states $|\Psi_{Bell}\rangle = \frac{1}{\sqrt{2}}(|00\rangle + e^{i\varphi}|11\rangle)$ for arbitrary values of the phase factor φ . Here 0 (1) denotes a zero-exciton (single exciton) QD, and the direct product of the quantum states $|jk\rangle \equiv |j\rangle \otimes |k\rangle$ form a four-dimensional basis in the Hilbert space $SU(2) \otimes SU(2)$. In the $J = 1$ subspace [23], $M \equiv \{-1, 0, 1\}$. We define $|M_1\rangle \equiv |J = 1, M = -1\rangle \equiv |0\rangle$, $|M_2\rangle \equiv |J = 1, M = 0\rangle \equiv |1\rangle$, and $|M_3\rangle \equiv |J = 1, M = 1\rangle \equiv |2\rangle$, as the vacuum of excitons, the single-exciton state and the biexciton state respectively. In the absence of light, we have:

$$E(J, M) = \Delta_\omega M + W[J(J+1) - M^2], \quad (9)$$

so the energy levels of the system are $E_0 \equiv E(1, -1) = W - \Delta_\omega$, $E_1 \equiv E(1, 0) = 2W$, and $E_2 \equiv E(1, 1) = W + \Delta_\omega$. Note that $E_{2,0} \equiv E_2 - E_0 = 2\Delta_\omega$ is unaffected by the interdot interaction strength W . Next, consider the action of the radiation pulse $\xi(t)$ over this pair of qubits; in the $J = 1$ subspace the Hamiltonian adopts the simple form:

$$\widehat{H}' = \begin{pmatrix} W - \Delta_\omega & \sqrt{2}A^* & 0 \\ \sqrt{2}A & 2W & \sqrt{2}A^* \\ 0 & \sqrt{2}A & W + \Delta_\omega \end{pmatrix}, \quad (10)$$

where $A \equiv |A| e^{i\phi}$ defines the real amplitude and the phase of the electron-photon coupling. Diagonalization gives the eigenenergies and eigenfunctions associated with Eq. (10). We get

$$E^3 - 4WE^2 + (5W^2 - 4|A|^2 - \Delta_\omega^2)E + 2W(\Delta_\omega^2 + 2|A|^2 - W^2) = 0, \quad (11)$$

as the eigenenergies equation. In resonance, $\Delta_\omega \equiv 0$, we find out that Eq. (11) has as its solutions:

$$E_0 = W, \text{ and } E_{1,2} = \frac{1}{2} \left(3W \pm \sqrt{16|A|^2 + W^2} \right). \quad (12)$$

On the other hand, if the pulse of light is an off-resonance one, we get the following eigenenergies:

$$E_0 = \frac{1}{6} \left\{ -2\alpha + \frac{2^{4/3}(\alpha^2 - 3\beta)}{\left(-2\alpha^3 + 9\alpha\beta - 27\gamma + \sqrt{-4(\alpha^2 - 3\beta)^3 + (2\alpha^3 - 9\alpha\beta + 27\gamma)^2}\right)^{1/3}} + \right. \\ \left. + 2^{2/3} \left(-2\alpha^3 + 9\alpha\beta - 27\gamma + \sqrt{-4(\alpha^2 - 3\beta)^3 + (2\alpha^3 - 9\alpha\beta + 27\gamma)^2} \right)^{1/3} \right\}, \quad (13)$$

$$E_1 = \frac{1}{12} \left\{ -4\alpha - \frac{i2^{4/3}(-i + \sqrt{3})(\alpha^2 - 3\beta)}{\left(-2\alpha^3 + 9\alpha\beta - 27\gamma + \sqrt{-4(\alpha^2 - 3\beta)^3 + (2\alpha^3 - 9\alpha\beta + 27\gamma)^2}\right)^{1/3}} + \right. \\ \left. + i2^{2/3}(i + \sqrt{3}) \left(-2\alpha^3 + 9\alpha\beta - 27\gamma + \sqrt{-4(\alpha^2 - 3\beta)^3 + (2\alpha^3 - 9\alpha\beta + 27\gamma)^2} \right)^{1/3} \right\}, \quad (14)$$

$$E_2 = \frac{1}{12} \left\{ -4\alpha + \frac{i2^{4/3}(i + \sqrt{3})(\alpha^2 - 3\beta)}{\left(-2\alpha^3 + 9\alpha\beta - 27\gamma + \sqrt{-4(\alpha^2 - 3\beta)^3 + (2\alpha^3 - 9\alpha\beta + 27\gamma)^2}\right)^{1/3}} - \right. \\ \left. - 2^{2/3}(1 + i\sqrt{3}) \left(-2\alpha^3 + 9\alpha\beta - 27\gamma + \sqrt{-4(\alpha^2 - 3\beta)^3 + (2\alpha^3 - 9\alpha\beta + 27\gamma)^2} \right)^{1/3} \right\}, \quad (15)$$

where, $\alpha = -4W$, $\beta = 5W^2 - 4|A|^2 - \Delta_\omega^2$, and $\gamma = 2W(2|A|^2 + \Delta_\omega^2 - W^2)$. Hence we find the following eigenfunctions for the $N = 2$ problem:

$$|E = E_k\rangle = \Gamma_k \left(|0\rangle + \frac{E_k + \Delta_\omega - W}{\sqrt{2}|A|} |1\rangle - \frac{2|A|^2 + (2W - E_k)(E_k + \Delta_\omega - W)}{2|A|^2} |2\rangle \right), \quad (16)$$

where $\Gamma_k = \sqrt{2}|A| \left[4|A|^2 + (\Delta_\omega + W)(E_k + \Delta_\omega - W) \right]^{-1/2}$, and $k = 0, 1, 2$. In the procedure described here, Eqs. (12)–(16) are necessary to perform the calculation of the laser pulses length required for generating the searched entangled Bell states.

In general, for any value of N , the total wave function associated to the initial condition $|\Psi(t=0)\rangle = |\Psi_0\rangle$ can be expressed as $|\Psi(t)\rangle_\Lambda = \sum_k C_k e^{-iE_k t} |\psi_k\rangle$, where $H' |\psi_k\rangle = E_k |\psi_k\rangle$, and $|\psi_k\rangle = \sum_j A_{kj} |M_j\rangle$. Here the normalization coefficients C_k [24] depend on the chosen initial condition $|\Psi_0\rangle$, the matrix elements A_{kj} must be determined for each particular value of N , and $|M_j\rangle \equiv |J, M_j; q\rangle$ as indicated in the precedent section. Hence, the total wave function $|\Psi(t)\rangle_\Lambda$ can be written as:

$$|\Psi(t)\rangle_\Lambda = \sum_k \sum_j C_k A_{kj} e^{-iE_k t} |M_j\rangle. \quad (17)$$

In the case of this section, $N = 2$ QDs, it is a straightforward exercise to compute the explicit coefficients of Eq. (17) for both of the J -subspaces that expand the Hilbert space $SU(2) \otimes SU(2)$. Next we will centre our attention on the discussion of finding the conditions to produce the maximally entangled Bell states. To perform that, we project the state $|\Psi_{Bell}\rangle$ over the wave function given by Eq. (17) getting the result:

$$\langle \Psi_{Bell} | \Psi(t) \rangle_{\Lambda} = \frac{1}{\sqrt{2}} \sum_k C_k (A_{k1} + e^{i\varphi} A_{k3}) e^{-iE_k t}. \quad (18)$$

Under the unitary evolution of the Hamiltonian H' , the density of probability $\wp(Bell)$ of finding the entangled Bell state in this coupled QDs system is proportional to $|\langle \Psi(t) \rangle_{\Lambda}|^2$; more explicitly we have that:

$$\wp(Bell) = \frac{1}{2} \left| \sum_k C_k (A_{k1} + e^{i\varphi} A_{k3}) e^{-iE_k t} \right|^2. \quad (19)$$

Results and discussion of the time evolution given by Eq. (19), for several different combinations of the physical parameters engaged in the model, are discussed later.

2. Coupling of $N=3$ QDs and Generation of GHZ States

Here we address the problem of generation of entangled GHZ states of the form $|\Psi_{GHZ}\rangle = \frac{1}{\sqrt{2}}(|000\rangle + e^{i\varphi}|111\rangle)$, for any φ , in the proposed system of 3 coupled QDs. In this case, the Hilbert space $SU(2)^{\otimes 3}$ is spanned by the eight basis vectors associated with the 3 different J -subspaces. Without loss of generality, consider the $J = \frac{3}{2}$ -subspace as the only one optically active. We introduce the notation $|M_1\rangle \equiv |3/2, -3/2\rangle \equiv |0\rangle$, $|M_2\rangle \equiv |3/2, -1/2\rangle \equiv |1\rangle$, $|M_3\rangle \equiv |3/2, 1/2\rangle \equiv |2\rangle$, and $|M_4\rangle \equiv |3/2, 3/2\rangle \equiv |3\rangle$ to mean the vacuum state, the single-exciton state, the biexciton state and the triexciton state, respectively. In the absence of light, the energy levels of the system are given by $E_0 \equiv E(3/2, -3/2) = \frac{3}{2}(W - \Delta_{\omega})$, $E_1 \equiv E(3/2, -1/2) = \frac{1}{2}(7W - \Delta_{\omega})$, $E_2 \equiv E(3/2, 1/2) = \frac{1}{2}(7W + \Delta_{\omega})$, and $E_3 \equiv E(3/2, 3/2) = \frac{3}{2}(W + \Delta_{\omega})$. We note that, as in the above case, the energy separation $E_{3,0} \equiv E_3 - E_0 = 3\Delta_{\omega}$ is unaffected by the interdot interaction strength

W . Now we consider the effect of the pulse of light $\xi(t)$ over this system of 3 QDs in the $J = \frac{3}{2}-$ subspace: the associated Hamiltonian is:

$$\widehat{H}' = \begin{pmatrix} \frac{3W}{2} - \frac{3\Delta_\omega}{2} & \sqrt{3}A^* & 0 & 0 \\ \sqrt{3}A & \frac{7W}{2} - \frac{\Delta_\omega}{2} & 2A^* & 0 \\ 0 & 2A & \frac{7W}{2} + \frac{\Delta_\omega}{2} & \sqrt{3}A^* \\ 0 & 0 & \sqrt{3}A & \frac{3W}{2} + \frac{3\Delta_\omega}{2} \end{pmatrix}. \quad (20)$$

Diagonalization leads us to the following 4th order equation:

$$\left(\left[\frac{3}{2}(W - \Delta_\omega) - E \right] \left[\frac{1}{2}(7W - \Delta_\omega) - E \right] - 3|A|^2 \right) \left(\left[\frac{3}{2}(W + \Delta_\omega) - E \right] \left[\frac{1}{2}(7W + \Delta_\omega) - E \right] - 3|A|^2 \right) - 4|A|^2 \left(\frac{3}{2}(W - \Delta_\omega) - E \right) \left(\frac{3}{2}(W + \Delta_\omega) - E \right) = 0, \quad (21)$$

which is too tedious to be analytically solved in the case of a pulse with an arbitrary frequency ω . However, if $\xi(t)$ is applied at resonance ($\Delta_\omega = 0$), we get the following eigenenergies:

$$E_{0,1} = \frac{5}{2}W + |A| \pm \sqrt{(W + |A|)^2 + 3|A|^2}, \text{ and } E_{2,3} = \frac{5}{2}W - |A| \pm \sqrt{(W - |A|)^2 + 3|A|^2}, \quad (22)$$

with eigenvectors:

$$|E_{0,1}\rangle = \eta_{0,1} \left[|0\rangle + \left(\frac{E_{0,1} - \frac{3W}{2}}{\sqrt{3}|A|} \right) |1\rangle + \left(\frac{E_{0,1} - \frac{3W}{2}}{\sqrt{3}|A|} \right) |2\rangle + |3\rangle \right], \quad (23)$$

$$|E_{2,3}\rangle = \eta_{2,3} \left[|0\rangle + \left(\frac{E_{2,3} - \frac{3W}{2}}{\sqrt{3}|A|} \right) |1\rangle - \left(\frac{E_{2,3} - \frac{3W}{2}}{\sqrt{3}|A|} \right) |2\rangle - |3\rangle \right], \quad (24)$$

where $\eta_i = \frac{1}{\sqrt{2}} \left(1 + \frac{(E_i - \frac{3W}{2})^2}{3|A|^2} \right)^{-\frac{1}{2}}$, $i = 0, \dots, 3$, are normalization constants. As it is well known, the associated total wave function $|\Psi(t)\rangle_\Lambda$ (Eq. (17)) depends on the chosen initial condition $|\Psi(t=0)\rangle \equiv |\Psi_0\rangle$ and is a linear combination of the eigenfunctions (23) and (24). We have computed, in both rotating and laboratory frames, the analytical expressions for $|\Psi(t)\rangle_\Lambda$ for all of the initial conditions $|\Psi_0\rangle = \{|0\rangle, |1\rangle, |2\rangle, |3\rangle\}$. As an example of this procedure, we give the result for the zero-exciton state as the initial state, i.e. $|\Psi_0\rangle = |M_1\rangle \equiv |0\rangle$. In this case, the wave function $|\Psi(t)\rangle_\Lambda$ is spanned by the following coefficients C_k and A_{kj} :

$$C_0 = \frac{E_1 - \frac{3W}{2}}{2\eta_0(E_1 - E_0)}, C_1 = \frac{E_0 - \frac{3W}{2}}{2\eta_1(E_0 - E_1)}, C_2 = \frac{E_3 - \frac{3W}{2}}{2\eta_2(E_3 - E_2)}, C_3 = \frac{E_2 - \frac{3W}{2}}{2\eta_3(E_2 - E_3)}; \quad (25)$$

$$\hat{A} \equiv \begin{pmatrix} \eta_0 & \frac{(E_0 - \frac{3}{2}W)e^{i\varphi}}{\sqrt{3}|A|}\eta_0 & \frac{(E_0 - \frac{3}{2}W)e^{i2\varphi}}{\sqrt{3}|A|}\eta_0 & e^{i3\varphi}\eta_0 \\ \eta_1 & \frac{(E_1 - \frac{3}{2}W)e^{i\varphi}}{\sqrt{3}|A|}\eta_1 & \frac{(E_1 - \frac{3}{2}W)e^{i2\varphi}}{\sqrt{3}|A|}\eta_1 & e^{i3\varphi}\eta_1 \\ \eta_2 & \frac{(E_2 - \frac{3}{2}W)e^{i\varphi}}{\sqrt{3}|A|}\eta_2 & -\frac{(E_2 - \frac{3}{2}W)e^{i2\varphi}}{\sqrt{3}|A|}\eta_2 & -e^{i3\varphi}\eta_2 \\ \eta_3 & \frac{(E_3 - \frac{3}{2}W)e^{i\varphi}}{\sqrt{3}|A|}\eta_3 & -\frac{(E_3 - \frac{3}{2}W)e^{i2\varphi}}{\sqrt{3}|A|}\eta_3 & -e^{i3\varphi}\eta_3 \end{pmatrix}. \quad (26)$$

The density of probability $\wp(GHZ)$ of finding the entangled GHZ state between vacuum and triexciton states is given by:

$$\wp(GHZ) = \frac{1}{2} \left| \sum_k C_k (A_{k1} + e^{i\varphi} A_{k4}) e^{-iE_k t} \right|^2. \quad (27)$$

Analytical and numerical computations have been performed for all of the initial conditions $|\Psi_0\rangle$ mentioned above. These results enable us to give specific conditions for the realization of such maximally GHZ entangled states starting from suitable φ -pulses and experimental parameters ϵ, W , and A . Details are discussed in section III.

B. The Numerical Description

The quantum dynamical problem given by Eq. (5) is easily expressed in terms of the expansion coefficients $d_M(t)$ of the wave function. As usual, we write $|\Psi(t)\rangle_\Lambda = \sum_{M=-J}^J d_M(t) e^{-iE_M t} |M\rangle$, so the time dependent problem is reduced to find the solutions of the following set of $2J + 1$ linear differential equations:

$$i\partial_t d_M(t) = A\sqrt{J(J+1) - M(M-1)} e^{(E_M - E_{M-1} - \omega)it} d_{M-1}(t) + A^* \sqrt{J(J+1) - M(M+1)} e^{(E_M - E_{M+1} + \omega)it} d_{M+1}(t), \quad (28)$$

where $E_M = E(J, M) + \omega$. More explicitly, $E_{M,M-1} \equiv E_M - E_{M-1} = \epsilon + W[1 - 2M]$, $E_{M,M+1} = W[1 + 2M] - \epsilon$, and the problem given by Eq. (28) can be expressed in terms of reduced units as follows:

$$i\partial_\tau f_M(\tau) = \lambda \sqrt{J(J+1) - M(M-1)} e^{[1+\mu(1-2M)-\nu]i\tau} f_{M-1}(\tau) + \lambda^* \sqrt{J(J+1) - M(M+1)} e^{-[1-\mu(1+2M)-\nu]i\tau} f_{M+1}(\tau), \quad (29)$$

where the dimensionless parameters $\lambda = \frac{A}{\epsilon}$, $\mu = \frac{W}{\epsilon}$, $\nu = \frac{\omega}{\epsilon}$, $\tau = \epsilon t$, and $d_M(t) = f_M(\tau)$ have been introduced. The set of Eqs. (29) gives the dynamics for any number of QDs and the (J, M) –set of values are defined as in section II.A. Numerical simulations were made varying the parameters λ , μ , and ν . Comparison of these numerical solutions with the analytical ones of the preceding section gives an excellent agreement in the generation of both Bell and GHZ states, starting from suitable initial conditions $|\Psi_0\rangle$. Results will be addressed in next section.

III. RESULTS AND DISCUSSION

In this section we shall discuss the main results obtained from the computation of both analytical and numerical solutions of the unitary evolution problem described in the precedent section. In Fig.1 we have plotted the density of probability of finding the entangled Bell state ($N = 2$) between vacuum and biexciton states given by Eq. (19) as a function of time for the initial condition $|\Psi_0\rangle = |0\rangle$. As it can be seen from Fig. 1, selective pulses of length τ_B can be used to create such maximally entangled Bell states in the system of two coupled QDs we have studied here. Numerical computations have been made in units of the gap energy ϵ . In this figure, the energy W is kept fixed whereas the amplitude of the radiation pulse A is varied. Results indicate that the time τ_B is increased with the diminishing of the incident field strength A . As an example, we consider wide-gap semiconductor QDs, like ZnSe based QDs, with band gap $\epsilon = 2.8$ eV and resonance optical frequency $\omega = 4.3 \times 10^{15}\text{s}^{-1}$. For a 0 or 2π –pulse, $W = 0.1$ and $A = \frac{1}{25}$, Fig. 1(a) shows that the density of probability for finding the QDs in the state $\frac{1}{\sqrt{2}}(|0\rangle + |2\rangle)$ require a pulse of length $\tau_B = 7.7 \times 10^{-15}\text{s}$. By changing the value of the parameter A , as it is plotted in Figs. 1(b), (c) and (d), we can modify the length of this Bell pulse to the required experimental conditions (Fig. 1 cover the interval $10^{-11}\text{s} < \tau_B < 10^{-15}\text{s}$). Another form of manipulating the length τ_B is shown in Fig. 2. Here we have varied the value of W for $A = 10^{-3}$ kept fixed. Experimentally, this variation of W can be tailored by changing the interdot distance. In this case, the

analysis shows that for a fixed value of A , the length τ_B diminishes with the diminishing of the interaction strength W .

The same manipulation of parameters proposed in Figs. 1 and 2 was done for the case of the entangled GHZ state ($N = 3$) between vacuum and triexciton states. In this case, we have plotted the density of probability given by Eq. (27) as a function of time, starting with the initial condition $|\Psi_0\rangle = |0\rangle$. Fig. 3 shows the selective pulses used to create such maximally entangled GHZ states in the system of three coupled QDs. For example, in the case of Fig. 3(a), the generation of the GHZ state $\frac{1}{\sqrt{2}}(|0\rangle + |3\rangle)$ requires the time $\tau_{GHZ} = 1.3 \times 10^{-14}$ s. Figs. 3(b), (c), and (d) explore several different ranges for the τ_{GHZ} -pulses required in the generation of such GHZ states. It is found that for W kept fixed, the time τ_{GHZ} is increased with the diminishing of the incident field strength A , and, on the other hand, for a fixed value of A , the length τ_{GHZ} diminishes with the diminishing of the interdot interaction strength.

The above results are not restricted to ZnSe-based QDs: by employing semiconductors of different bandgap ϵ (GaAs, for instance), other regions of parameter space can be explored. We have studied the time evolution of the system of QDs for several different values of the phase φ , getting similar results if compared with the ones discussed before. We only include the 0 or 2π -pulses results since they are the desired ones for the discussion given in Section IV. The relevant experimental conditions as well as the required coherent control to realize the above combinations of parameters are compatible with those demonstrated in [13]. We point out that the procedure described in this paper is valid for any value of the phase constant φ , in contrast with a recent work by two of us [21], where analytic results were derived for the particular case $\varphi = \frac{\pi}{2}$. The generation of maximally entangled states given in this paper has considered the experimental situation of global laser pulses only; however, by using near-field optical spectroscopy [15], individual QDs can be addressed from an entire ensemble of QDs by using local pulses, fact that can be exploited in the generation of entangled states with different symmetries, such as the antisymmetric one

$\frac{1}{\sqrt{2}}(|01\rangle - |10\rangle)$. By doing this, we can be able to perform the famous Bell basis of four mutually orthogonal states for the 2 qubits, all of which are maximally entangled, *i.e.*, the set of states $\frac{1}{\sqrt{2}}\{(|00\rangle + |11\rangle), (|00\rangle - |11\rangle), (|01\rangle + |10\rangle), (|01\rangle - |10\rangle)\}$. From a general point of view, this basis is of fundamental relevance for quantum information processing. We stress that the optical generation of excitonic entangled states in coupled QDs given here could be exploited in solid state devices to perform quantum protocols, as recently proposed in [25] for teleporting an excitonic state in a coupled QDs system.

IV. COUPLED DOTS AND QUANTUM INFORMATION PROCESSING

To perform quantum computation operations, we require an initial pure state and after that, a series of transformations of this state using unitary operations. Another possibility to perform these operations is by using an initial mixed state, providing the decoherence time is sufficiently long [10]. In order to implement such quantum operations we need two elements: the *Hadamard* transformation and the quantum CNOT gate. In the orthonormal computation basis of single qubits $\{|0\rangle, |1\rangle\}$, the CNOT gate acts on two qubits $|\varphi_i\rangle$ and $|\varphi_j\rangle$ simultaneously as follows: $\text{CNOT}_{ij}(|\varphi_i\rangle|\varphi_j\rangle) \mapsto |\varphi_i\rangle|\varphi_i \oplus \varphi_j\rangle$. Here \oplus denotes *addition modulo 2*, and the indices i and j refer to the control bit and the target bit respectively. The Hadamard transformation H^T acts only on single qubits by performing the rotations: $H^T(|0\rangle) \mapsto \frac{1}{\sqrt{2}}(|0\rangle + |1\rangle)$, and $H^T(|1\rangle) \mapsto \frac{1}{\sqrt{2}}(|0\rangle - |1\rangle)$. We also introduce a pure state $|\mathbb{N}\rangle$ in this Hilbert space given by $|\mathbb{N}\rangle = u|0\rangle + v|1\rangle$, with $|u|^2 + |v|^2 = 1$, where u and v are complex numbers. In our scheme, $|0\rangle$ represents the vacuum state for excitons while $|1\rangle$ represents a single exciton. Demonstration of single qubit rotations (and hence the Hadamard transformation) in the case of individual excitons confined to QDs is expected since a very recent experimental work has reported direct observation of excitonic Rabi oscillations in semiconductor quantum wells [26]. Despite the fact that Rabi Flopping in QDs is still under intensive experimental search, results given in [26] lead us to think that we are not too far away from the experimental observation of such excitonic Rabi oscillations

in QDs and hence of the demonstration of single qubit operations.

The adequate preparation, computation and readout, in addition to the coherent coupling of the qubits to the environment are compulsory steps for the successful construction of an universal quantum computer. We review these requirements and their relationship with the model proposed here:

1. *A very well defined Hilbert Space:* We must to have an adequate control over the Hilbert space of qubits. In our scheme, the orthonormal computation basis of single qubits is represented by the vacuum state ($|0\rangle$) and the single state of excitons ($|1\rangle$).
2. *Initializing the computer:* Before commencing any quantum computation task, we need to be able for a rapid relaxing process of our qubits to their ground state, i.e. zero exciton per dot. In our case, numerical values indicate that this state is gained by turning the laser off and waiting for a few femtoseconds.
3. *Inputting initial data and Readout:* As pure and entangled states with different symmetries can be obtained by using experimental techniques described in [13–15], we have the ability to manipulate the input of the quantum state of the QDs system. Hence, we have the experimental possibility to control the optical excitation and to detect individual QD signals from an entire dot ensemble, facilitating the individual qubit control for the readout. In fact, nanoprobeing enables us to measure directly the excitonic and biexcitonic luminescence from single QDs [15].
4. *Universal set of Gate Operations:* We need the ability to perform single qubit rotations and two qubit gates. We stress that the generation of the maximally entangled states shown in Figs. 1 – 3 corresponds to the physical realization of a Hadamard transform followed by a CNOT operation in the Bell case, and 2 CNOT operations in the GHZ case. As to the practical semiconductor nanostructures implementation, this set of gate operations is in a preliminary stage of investigation and demands intensive experimental study.

5. *Decoherence and the Coupling to the Environment:* By taking into account decoherence mechanisms (exciton-acoustic-phonon type) on the process of generation of the entangled states discussed here, a recent work by Rodríguez *et al.* [27] has shown that this generation is preserved over a reasonable parameter window, giving the possibility of performing the unitary transformations required for quantum computing before decoherence of the excitonic states takes place.

V. CONCLUSIONS

In summary, we have solved both analytically and numerically the quantum state equation of motion for excitons in two and three coupled QD systems driven by classical pulses of light. By doing this, we have shown a mechanism for preparing maximally entangled Bell and GHZ states via excitons in optically-driven QDs, exploiting current levels of coherent optical control such as the ones demonstrated by using ultra-fast spectroscopy [13,14], and near-field optical spectroscopy [15]. This mechanism enables us to the generation of single qubit rotations, such as the Hadamard one, and quantum CNOT gates. In particular, the procedure presented here lead us to the generation of the whole Bell basis, a fact that can be exploited in the process of quantum teleportation of excitonic states in systems of coupled QDs [25]. Furthermore, by taking into account the main decoherence mechanisms, such as the exciton-acoustic-phonon one, this optical generation of quantum entanglement is preserved over a reasonable parameter window leading, in principle, to the possibility of performing several hundred quantum computation operations before decoherence of these excitonic states takes place.

The authors acknowledge the support of COLCIENCIAS. J.H.R. thanks the hospitality and support of the ESF-QIT programme meeting 1999 in Cambridge, where part of this work has been done.

REFERENCES

- [1] R.P. Feynman, *Int. J. Theor. Phys.* **21**, 467 (1982), *Opt. News* **11**, 11 (1985).
- [2] D. Deutsch, *Proc. R. Soc. London A* **400**, 97 (1985).
- [3] W.K. Wootters and W.H. Zurek, *Nature* **299**, 802 (1982); N.D. Mermin, *Physics Today* **38** 4, 38 (1985); W.H. Zurek, *ibid.* **44** 10, 36 (1991); C.H. Bennett, *ibid.* **48** 10, 24 (1995); articles in the special issue on quantum information, *Physics World*, March 1998; A. Ekert and R. Jozsa, *Rev. Mod. Phys.* **68**, 733 (1996).
- [4] A.K. Ekert, *Phys. Rev. Lett.* **67**, 661 (1991); C.H. Bennett, G. Brassard, and N.D. Mermin, *ibid.* **68**, 557 (1992); C.H. Bennett, G. Brassard, and A. Ekert, *Scientific American* **267** 4, 26 (1992).
- [5] C.H. Bennett, G. Brassard, C. Crépeau, R. Jozsa, A. Peres, and W.K. Wootters, *Phys. Rev. Lett.* **70**, 1895 (1993).
- [6] P.W. Shor, in *Proceedings of the 35th Annual Symposium on the Foundations of Computer Science*, ed. by S. Goldwasser (IEEE Computer Society, Santa Fe, Los Alamitos, CA), 124 (1994).
- [7] P.W. Shor, *Phys. Rev. A* **52**, 2493 (1995); A.M. Steane, *Phys. Rev. Lett.* **77**, 793 (1996).
- [8] J.I. Cirac and P. Zoller, *Phys. Rev. Lett.* **74**, 4091 (1995); C. Monroe, D.M. Meekhof, B.E. King, W.M. Itano, and D.J. Wineland, *ibid.* **75**, 4714 (1995).
- [9] Q.A. Turchete, C.J. Hood, W. Lange, H. Mabuchi, and H.J. Kimble, *Phys. Rev. Lett.* **75**, 4710 (1995).
- [10] N.A. Gershenfeld and I.L. Chuang, *Science* **275**, 350 (1997); D.G. Cory, A.F. Fahmy, and T.F. Havel, *Proc. Natn. Acad. Sci. USA* **94**, 1634 (1997); E. Knill, I.L. Chuang, and R. Laflamme, *Phys. Rev. A* **57**, 3348 (1998); J.A. Jones, M. Mosca, and R.H. Hansen, *Nature* **393**, 344 (1998).

[11] A. Shnirman, G. Schön, and Z. Hermon, Phys. Rev. Lett. **79**, 2371 (1997); D.V. Averin, Solid State Commun. **105**, 659 (1998); Y. Makhlin, G. Schön, and A. Shnirman, Nature **398**, 305 (1999).

[12] A. Barenco, D. Deutsch, A. Ekert, and R. Jozsa, Phys. Rev. Lett. **74**, 4083 (1995); B.E. Kane, Nature **393**, 133 (1998); G. Burkard, D. Loss, and D.P. DiVincenzo, Phys. Rev. B **59**, 2070 (1999); A. Imamoglu, D.D. Awschalom, G. Burkard, D.P. DiVincenzo, D. Loss, M. Sherwin, and A. Small, Phys. Rev. Lett. **83**, 4204 (1999); R. Vrijen, E. Yablonovitch, K. Wang, H.W. Jiang, A. Balandin, and D.P. DiVincenzo, quant-ph/9905096.

[13] N.H. Bonadeo, J. Erland, D. Gammon, D.S. Katzer, D. Park, and D.G. Steel, Science **282**, 1473 (1998).

[14] N.H. Bonadeo, G. Chen, D. Gammon, D.S. Katzer, D. Park, and D.G. Steel, Phys. Rev. Lett. **81**, 2759 (1998).

[15] A. Chavez-Pirson, J. Temmyo, H. Kamada, H. Gotoh, and H. Ando, Appl. Phys. Lett. **72**, 3494 (1998).

[16] J.S. Bell, Physics **1**, 195 (1964).

[17] A. Einstein, B. Podolsky, and N. Rosen, Phys. Rev. **47**, 777 (1935).

[18] D.M. Greenberger, M.A. Horne, and A. Zeilinger, in *Bell's Theorem, Quantum Theory and Conceptions of the Universe*, ed. M. Kafatos, pp. 73, Kluwer, Dordrecht, The Netherlands (1989); D.M. Greenberger, M.A. Horne, A. Shimony, and A. Zeilinger, Am. J. Phys. **58**, 1131 (1990).

[19] A. Aspect, J. Dalibard, and G. Roger, Phys. Rev. Lett. **49**, 1804 (1982).

[20] Throughout this paper we refer to this phase factor as the “ φ –pulse”, to recognize the kind of entangled state generated in the optical process.

[21] L. Quiroga and N.F. Johnson, Phys. Rev. Lett. **83**, 2270 (1999).

[22] Here we express the Hamiltonian H with accuracy of the constant term $\frac{W}{2} \sum_p \{c_p^\dagger c_p + h_p h_p^\dagger\} = \frac{WN}{2}$.

[23] Note that in general, for $J = \frac{N}{2}$, the multiplicity $D_J = 1$, hence q is irrelevant.

[24] Let us write $|\Psi(0)\rangle = \sum_k \beta_k |M_k\rangle$ ($\beta_k = \langle M_k | \Psi(0) \rangle$). From the expansion given for $|\Psi(t)\rangle_\Lambda$ it follows that $|\Psi(0)\rangle = \sum_k C_k |\psi_k\rangle$, hence the general expression for the coefficients C_k becomes $C_k = \langle \psi_k | \Psi(0) \rangle = \sum_j \beta_j \langle \psi_k | M_j \rangle = \sum_j \beta_j A_{kj}^*$.

[25] J.H. Reina and N.F. Johnson, cond-mat/9906034.

[26] A. Schülzgen, R. Binder, M.E. Donovan, M. Lindberg, K. Wundke, H.M. Gibbs, G. Khitrova, and N. Peyghambarian, Phys. Rev. Lett. **82**, 2346 (1999).

[27] F.J. Rodríguez, L. Quiroga, and N.F. Johnson, cond-mat/9909139.

Figure Captions

FIG. 1. Generation of Bell States. These pulses correspond to the realization of the Hadamard gate followed by a quantum CNOT gate. $W = 0.1$, $\varphi = 0$, and (a) $A = \frac{1}{25}$, (b) $A = \frac{1}{50}$, (c) $A = 10^{-2}$, and (d) $A = 10^{-3}$. In the plots 1 – 3, $|\Psi(t)\rangle$ denotes the total wavefunction of the system at time t in both laboratory (solid curves) and rotating frames (dashed curves).

FIG. 2. Generation of Bell states. $A = 10^{-3}$, $\varphi = 0$, and (a) $W = 0.1$, (b) $W = 0.05$, and (c) $W = 10^{-2}$.

FIG. 3. Generation of GHZ states. These pulses correspond to the realization of the Hadamard gate followed by two quantum CNOT gates. $W = 0.1$, $\varphi = 0$, and (a) $A = \frac{1}{25}$, (b) $A = \frac{1}{50}$, (c) $A = 10^{-2}$, and (d) $A = 10^{-3}$.

Figure 1

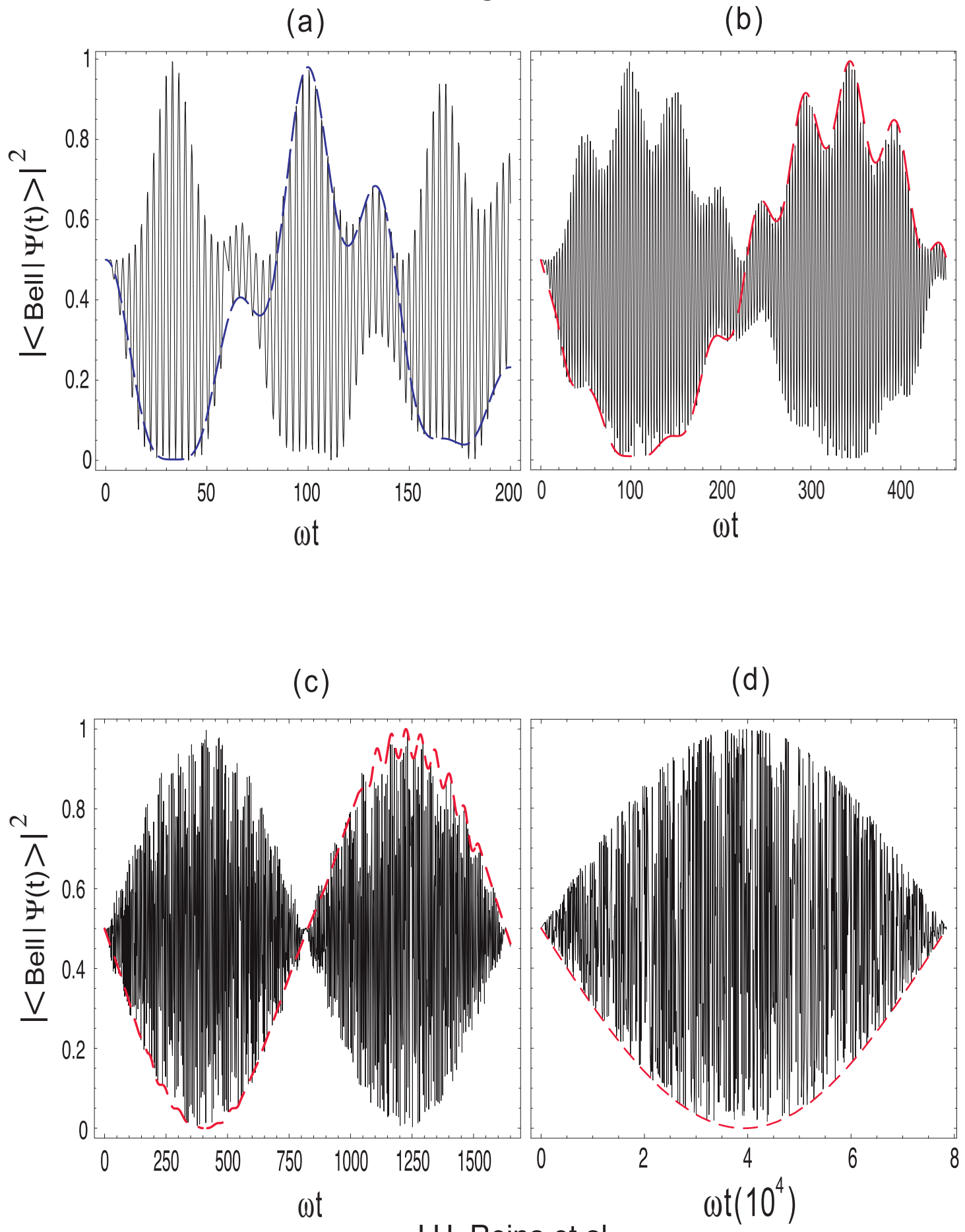


Figure 2

J.H. Reina et al.

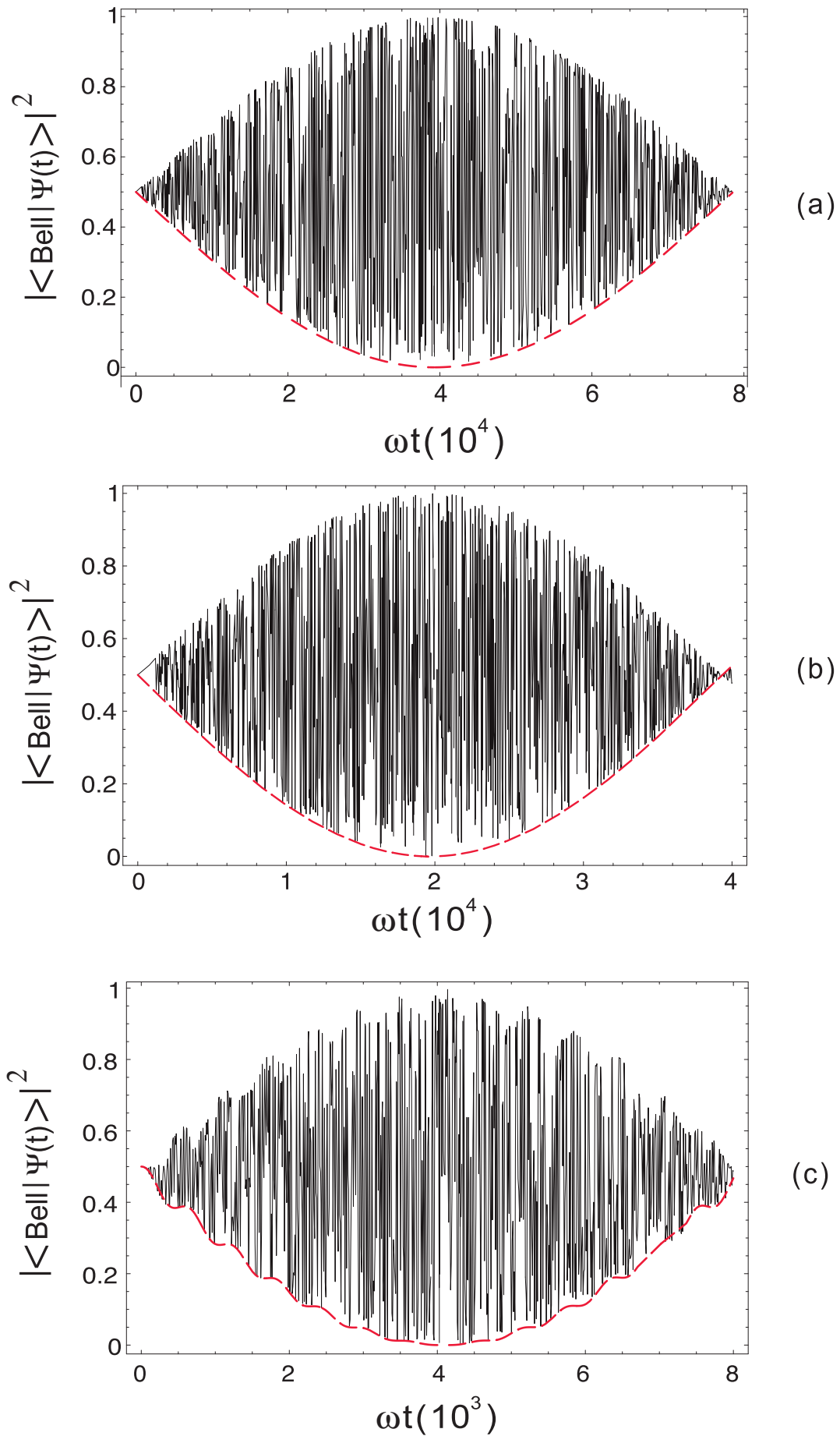


Figure 3

